

Model for hypernucleus production in heavy ion collisions

V. Topor Pop and S. Das Gupta¹

¹*Physics Department, McGill University, Montréal, Canada H3A 2T8*

(Dated: October 9, 2018)

We estimate the production cross sections of hypernuclei in projectile like fragment (PLF) in heavy ion collisions. The discussed scenario for the formation cross section of Λ hypernucleus is: (a) Λ particles are produced in the participant region but have a considerable rapidity spread and (b) Λ with rapidity close to that of the PLF and total momentum (in the rest system of PLF) up to Fermi motion can then be trapped and produce hypernuclei. The process (a) is considered here within Heavy Ion Jet Interacting Generator (HIJING/B \bar{B}) model and the process (b) in the canonical thermodynamic model (CTM). We estimate the production cross sections for a hypernucleus ${}^A_Z\Lambda$ where $Z = 1, 2, 3$ and 4 for C + C at total nucleon-nucleon center of mass (c.m.) energy $\sqrt{s_{NN}} = 3.7$ GeV, and for Ne+Ne and Ar+Ar collisions at $\sqrt{s_{NN}} = 5.0$ GeV. By taking into account explicitly the impact parameter dependence of the colliding systems, it is found that the cross section is different from that predicted by the coalescence model and large discrepancy is obtained for ${}^9_\Lambda\text{He}$ and ${}^9_\Lambda\text{Be}$ hypernuclei.

PACS numbers: 25.75.-q, 21.80.+a, 25.70Mn, 25.70Pq

I. INTRODUCTION

Hypernuclear production in reactions between heavy nuclei was first theoretically proposed by Kerman and Weiss [1]. They found that relativistic heavy ion collisions (rHIC) offer the best possibility to create exotic finite nuclear system with finite strangeness. However, the experimental results have so far been rather limited due to short lifetime of hypernuclei [2–4], which impedes their detection. Since the mechanism of the heavy ion induced hypernuclear reaction is not well understood, this field of research attracted mainly theoretical interest, see, e.g., Refs. [5–21].

The future experimental projects as planned at the Facility for Anti-protons and Ion Research (GSI-FAIR, Germany) [22–27] and the Nuclotron-based Ion Collider Facility (NICA), at Joint Institute for Nuclear Research (JINR), Dubna, Russia [28], aim to look for light proton/neutron rich exotic hypernuclei, and to extend their study to heavier hypernuclei (which can be produced only in rHIC), toward protons and neutron drip lines. In addition, there are special light hypernuclei of interest, whose properties are dictated by their unusual structure [29], e.g., nuclei with the hyperon halo (${}^3_\Lambda\text{H}$); neutron-rich hypernuclei; nuclei with an unstable core, where the hyperon is a sort of “*glue*” ensuring stability (${}^6_\Lambda\text{H}$, ${}^6_\Lambda\text{He}$, ${}^8_\Lambda\text{He}$). Recently at RHIC BNL (Relativistic Heavy Ion Collider at Brookhaven National Laboratory) the observation of (anti)hypertritons has been reported in nuclear collisions [30],[31].

The research program at the SPS CERN-Geneva (Super Proton Synchrotron at European Organization for Nuclear Research) and at RHIC BNL will cover the energy range $\sqrt{s_{NN}} = 5$ -50 GeV from below up to well above the energy of the onset of deconfinement (expected approximately at $\sqrt{s_{NN}} = 6$ -8 GeV). Moreover, HypHI-collaboration [22, 23] and the project Multi-Purpose Detector (MPD/NICA) [28] will cover the relevant energies

$\sqrt{s_{NN}} = 2.7$ -9.4 GeV. These experiments aim to measure the production of hypernuclei in energetic collisions between light nuclei, since their identification via the weak decay of the hyperon into pion is much easier for such systems.

In this paper a hybrid model based on participant-spectator picture and combined with canonical thermodynamic (CTM) model is used to determine, in high energy heavy-ion collisions, the probability of forming a hypernucleus and to estimate its production cross section. For rHIC in 3-10 GeV energy range the following scenario (supported by experiments) applies. For a general impact parameter there is a region of violent collision called the participating region. In addition, there is a mildly excited projectile like fragment (PLF) and also a mildly excited target like fragment (TLF). Physics of both PLF and TLF are similar for symmetric collisions; here we concentrate our analysis on PLF. Because of excitation energy (usually characterized by a temperature, T) PLF will break up into many fragments and the velocities of these fragments are centered around the velocity of the projectile. In fixed target experiments they are emitted in a forward cone and are more easily recognizable. In the participating region, apart from original neutrons and protons, others particles (pions, kaons, Λ 's, etc.) are produced. The produced Λ particles have an extended rapidity range. Those produced in the rapidity range close to that of the projectile and having total momenta in the PLF frame up to Fermi momentum ($p_{\text{tot}} < 250$ MeV/c) can be trapped in the PLF and form hypernuclei. The present problem has also been analyzed previously (see Refs. [5, 6, 11, 12]) at lower $\sqrt{s_{NN}}$ energies ($\sqrt{s_{NN}} = 2.7$ -3.1 GeV). This work is in a similar spirit but at higher c.m. energy and uses different models for (a) Λ particles production in the participant region taking into consideration impact parameter dependence of the specific collision and (b) attachment of the Λ particle to different fragments in the PLF forming what we refer

here as composite. It is felt that in view of the future experimental activities [22–28] the results from alternative models, and at different energies, will help to better establish the mechanism for formation of hypernuclei.

Our calculations are performed in two separate stages. For a given impact parameter (b) a large number of events ($10^5 - 10^7$) are generated with HIJING/B \bar{B} model in order to obtain the average number of Λ particles per event ($\langle n_\Lambda(b) \rangle$) within appropriate kinematic cuts in rapidity and momentum. Within the model we can also calculate the average number of the nucleons in the PLF, $\langle n_{\text{PLF}} \rangle = \langle n_1(b) \rangle + \langle n_2(b) \rangle$, where $n_1(b)$ stands for neutrons, and $n_2(b)$ for protons.

We can characterize a produced composite (with and without strangeness) by three symbols: a , z and h , where a is the atomic mass, z is the charge value of the isotope, and h refers to the number of hyperons embedded into the nucleus (a , z). For $h = 0$ we have normal composites. For $h = 1$ we have a hypernucleus with one Λ . It is also possible to include the case $h = 2$ (i.e., ${}^a_{\Lambda\Lambda}z$). Similarly it is possible to include other kinds of hyperons, i.e., Σ . However, this is beyond the scope of the present work. Calculations using canonical thermodynamic model (CTM) [20, 32, 33] are performed in the second stage to estimate the average number ($\langle n_{a,z,1}(b) \rangle$) of hypernuclei (${}^a_{\Lambda}z$) produced at a given temperature T , when the PLF has one Λ , and the average number of nucleons $\langle n_{\text{PLF}} \rangle = \langle n_1(b) \rangle + \langle n_2(b) \rangle$.

There are two major approximations in our approach: (i) the time dependence of source function for hyperons and fragments has been neglected; (ii) we neglect also secondary hypernuclear processes. The transport calculations predict only moderate contributions [21] to the total hyper-fragment cross section from indirect coalescence through the πB channel (where B stands for a baryon and π for a pion). With these assumptions, the formation cross section of a hypernucleus in the PLF rest system can be expressed by:

$$\sigma_\Lambda^{(A_F Z)} = \int 2\pi b db \langle n_\Lambda(b) \rangle \langle n_{a,z,1}(b) \rangle \quad (1)$$

The basic outline and main parameters of HIJING/B \bar{B} model are presented in Sec. II. We employ reasonable theoretical evaluations for the Λ particle production with specific kinematic cuts. In Sec. III we give details of CTM calculations. The results and the discussions are presented in Sec. IV. The final conclusions are summarized in Sec. V.

II. OUTLINE OF HIJING/B \bar{B} V2.0 MODEL.

The HIJING [34] and HIJING/B \bar{B} v1.10 models [35] have been used extensively to determine the physical properties of the matter produced in rHIC and to study particle production. String models describe the collisions

through the exchange of color or momentum between partons in the projectile and target. As a consequence of these exchanges, these partons become joined by colorless objects, which are called string, ropes or flux tubes. In HIJING type models [34] the soft beam jet fragmentation is modeled by diquark-quark strings with gluon kinks induced by soft gluon radiations. Hard collisions are included within perturbative Quantum Chromodynamics (pQCD) computed parton-parton collisions. The mini-jets physics is embedded via an eikonal multiple collision framework using pQCD to compute the initial and final state radiation and hard scattering rates. The cross section for hard parton scatterings is enhanced by a factor $K=2$ in order to simulate high order corrections. The HIJING model was originally designed for hadron-hadron interactions. Generalization to hadron-nucleus ($p + A$) and nucleus-nucleus ($A + A$) collisions is performed [34] through the Glauber theory. Besides the Glauber nuclear eikonal extension, shadowing of nuclear parton distributions is modeled. In addition, dynamical energy loss of the (mini)jets is taken into account through an effective dE/dx (approximately 2 GeV/fm per gluon mini-jet). These models contain a *soft* and a *hard* component, which is crucial for their application from FAIR to Large Hadron Collider (LHC) energies.

Unlike conventional di-quark fragmentation implemented in HIJING model [34], a baryon junction allows the di-quark to split with the three independent flux lines tied together at a junction in HIJING/B \bar{B} v1.10 [35]. We introduce [36] a new version (v2.0) of HIJING/B \bar{B} that differs from HIJING/B \bar{B} v1.10 [35] in its implementation of hypothesized junction anti-junction (J \bar{J}) loops. A picture of a junction loop is as follows: a color flux line splits at some intermediate point into two flux line at one junction and then the flux line fuse back into one at a second anti-junction somewhere further along the original flux line. Before fragmentation, we compute the probability that a junction loop occurs in the string. The probability of such loop is assumed to increase with the number of binary interactions that the incident baryon suffers in passing through the oncoming nucleus [36]. This number depends on the impact parameter and is computed in HIJING using eikonal path through a diffuse nuclear density. Moreover, we add an enhanced intrinsic (anti)di-quark p_T kick in any standard (q-qq) strings that should contain one or multiple J \bar{J} loops. This mechanism correspond to some degree of *collectivity* for parton interactions.

In string fragmentation phenomenology, it has been proposed that the strong enhancement of strange particle observables require strong color field (SCF) effects [37]. The particle production is large and dominated by pair production and the energy density appears to exceed the one required for quark gluon plasma (QGP) formation. The overall scenario is consistent with particle production from a strong color field (SCF), formation of a QGP and subsequent hadronization. The SCF effects are also possible source of novel *baryon/hyperon physics*. In our previous works [38–41], we explore with HIJING/B \bar{B} v2.0

model calculations, possible dynamical effects associated with long-range coherent field (SCF), that may arise in rHIC. These analysis point to the *need for collective motion*, together with *high initial-state energy densities*.

For a uniform chromoelectric flux tube with field (E) the pair production rate [42] per unit volume for a heavy quark is given by:

$$\Gamma = \frac{\kappa^2}{4\pi^3} \exp\left(-\frac{\pi m_Q^2}{\kappa}\right) \quad (2)$$

where for strange quark $Q = s$, the current quark mass is in the range of $m_s = 80 - 190$ MeV and the constituent quark mass $M_s = 350$ MeV (for detailed discussion see Ref. [39]). Note that $\kappa = |eE|_{eff} = \sqrt{C_2(A)/C_2(F)} \kappa_0$ is the effective string tension in terms of the vacuum string tension $\kappa_0 \approx 1$ GeV/fm and $C_2(A)$, $C_2(F)$ are the second order Casimir operators (see Ref. [37]). A measurable rate for spontaneous pair production requires “strong chromo electric fields”, such that $\kappa/m_Q^2 > 1$ at least some of the time. On the average, longitudinal electric field “string” models predict for heavier flavor a very suppressed production rate per unit volume γ_Q via the well known Schwinger formula [42], since

$$\gamma_{Q\bar{Q}} = \frac{\Gamma_{Q\bar{Q}}}{\Gamma_{q\bar{q}}} = \exp\left(-\frac{\pi(m_Q^2 - m_q^2)}{\kappa_0}\right) \ll 1 \quad (3)$$

for $Q = s$ and $q = u, d$. For a color rope on the other hand, if the *average* string tension value ($\langle \kappa \rangle$) increases from 1.0 GeV/fm to 2.0-3.0 GeV/fm, the rate Γ for strangeness pairs to tunnel through the longitudinal field increases (see Refs. [38, 39]).

We take into account SCF in our model by an *in medium effective string tension* $\kappa > \kappa_0$, which lead to new values for the suppression factors, as well as the new effective intrinsic transverse momentum k_T . This includes: i) the ratio of production rates of di-quark to quark pairs (di-quark suppression factor), $\gamma_{qq} = P(qq\bar{q}\bar{q})/P(q\bar{q})$, ii) the ratio of production rates of strange to non-strange quark pairs (strangeness suppression factor), $\gamma_s = P(s\bar{s})/P(q\bar{q})$, iii) the extra suppression associated with a diquark containing a strange quark compared to the normal suppression of strange quark (γ_s), $\gamma_{us} = (P(us\bar{u}\bar{s})/P(ud\bar{u}\bar{d})) / (\gamma_s)$, iv) the suppression of spin 1 diquarks relative to spin 0 ones (apart from the factor of 3 enhancement of the former based on counting the number of spin states), γ_{10} , and v) the (anti)quark ($\sigma_q'' = \sqrt{\kappa/\kappa_0} \cdot \sigma_q$) and (anti)di-quark ($\sigma_{qq}'' = \sqrt{\kappa/\kappa_0} \cdot f \cdot \sigma_{qq}$) Gaussian width.

In this paper we extend our study in the framework of HIJING/B \bar{B} v2.0 model [39] to strange particle production at the FAIR and MPD/NICA energy range ($\sqrt{s_{NN}} = 2.7-9.4$ GeV). The experimental situation has so far been rather poor for measurements of strange particles at forward rapidities, due to limited acceptances of the detectors. The very forward rapidity (closer to projectile rapidity) are dealt with by models only. Using HIJING/B \bar{B} v2.0 model we analyze the production of the

TABLE I: Main parameters used in symmetric $A+A$ collisions. The parameters are defined in the text. Set 1 correspond to calculations without JJ loops and SCF effects. Set 2 and 3 include both effects and correspond to different mean values of the string tension.

A + A	κ (GeV/fm)	γ_{qq}	γ_s	γ_{us}	γ_{10}	σ_q (GeV/c)	f
Set 1	$\kappa_0 = 1.0$	0.02	0.30	0.40	0.05	0.350	1
Set 2	$\kappa_2 = 2.0$	0.14	0.55	0.63	0.12	0.495	3
Set 3	$\kappa_3 = 3.0$	0.27	0.67	0.74	0.18	0.606	3

average value per event $\langle n_\Lambda(b) \rangle$ with specific kinematic cuts in rapidity $(y_{proj} - 0.05) \leq \delta y \leq (y_{proj} + 0.05)$, (where y_{proj} stands for projectile rapidity) and total momentum $p_{tot} < 250$ MeV/c in the PLF rest system, which can leads to the formation of hypernucleus in rHIC. The main parameters used in the calculations presented here are given in Table I.

In these calculations we do not consider nuclear effects such as shadowing and quenching [34], [36], which are specific only for very high energy interactions ($\sqrt{s_{NN}} \geq 20$ GeV). Within our model we do not include rescattering processes which Relativistic Quantum Molecular Dynamics (RQMD) model calculations [43] show to be negligible at the forward rapidity. The physics embedded in our model include a “hard” (pQCD) and an underlying “soft” part, therefore we can not apply our phenomenology for energies $\sqrt{s_{NN}} \leq 3.0$ GeV. The detailed analysis for (multi)strangeness production from FAIR to SPS and RHIC energies within HIJING/B \bar{B} v2.0 model will be presented elsewhere [44].

For a given impact parameter (b) we calculate with HIJING/B \bar{B} v2.0 model the average number per event $\langle n_\Lambda(b) \rangle$, in appropriate kinematic phase space, and the average number of nucleons in the PLF, $\langle n_{PLF}(b) \rangle$. The predictions for transverse momentum (p_T) spectra of Λ particles with rapidity cut δy for symmetric colliding systems $^{12}\text{C} + ^{12}\text{C}$, $^{20}\text{Ne} + ^{20}\text{Ne}$, and $^{40}\text{Ar} + ^{40}\text{Ar}$ at $\sqrt{s_{NN}} = 5$ GeV are presented in Fig. 1 for central ($b = 3$ fm, left panel) and peripheral ($b = 6$ fm, right panel). The values of the parameters used to obtain the results discussed here, are Set 2 from Table I.

The average value per event $\langle n_\Lambda(b) \rangle$ within rapidity cut δy and with total momentum ($p_{tot} < 250$ MeV/c) in the projectile rest system, are given in Table II for the symmetric colliding system $^{12}\text{C} + ^{12}\text{C}$, $^{20}\text{Ne} + ^{20}\text{Ne}$ and $^{40}\text{Ar} + ^{40}\text{Ar}$. These numbers are the main input in Eq. 1 used to calculate inclusive cross sections for the formation of hypernuclei in nucleus-nucleus collisions in the PLF rest frame.

Our estimate for total number of events with one Λ particle produced in the projectile rapidity region in C + C collisions at $\sqrt{s_{NN}} = 3.7$ GeV is 13.05×10^{-4} . A comparable value (26.6×10^{-4}) at lower energy (2A GeV in laboratory system), is obtained [23] with ultrarelativistic quantum molecular dynamics (UrQMD) calculations by

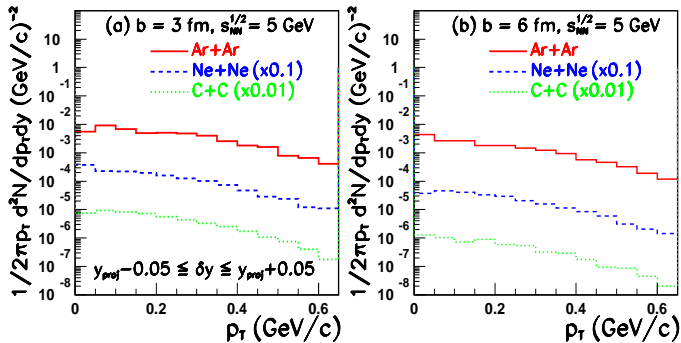


FIG. 1: (color online). The HIJING/B \bar{B} v2.0 model predictions for p_T spectra of Λ s particle within rapidity cut δy at $\sqrt{s_{NN}} = 5$ GeV. For clarity the values for Ne + Ne and C + C are multiplied by 0.1 and 0.01 respectively.

TABLE II: The dependence on the impact parameter (b) of the mean number of Λ 's per event ($\langle n_{\Lambda}(b) \rangle$) obtained within kinematic cuts (see Sec. II) in the PLF rest frame for symmetric colliding systems: $^{12}\text{C} + ^{12}\text{C}$, $^{20}\text{Ne} + ^{20}\text{Ne}$ and $^{40}\text{Ar} + ^{40}\text{Ar}$.

$\sqrt{s_{NN}}$	C + C	Ne + Ne	Ar + Ar
	3.7 GeV	5.0 GeV	5.0 GeV
b (fm)	$\langle n_{\Lambda}^{\text{C}}(b) \rangle \times 10^4$	$\langle n_{\Lambda}^{\text{Ne}}(b) \rangle \times 10^4$	$\langle n_{\Lambda}^{\text{Ar}}(b) \rangle \times 10^4$
0.0	4.61	6.70	16.4
1.0	2.80	6.00	16.20
2.0	3.01	5.60	18.90
3.0	1.44	5.20	15.80
4.0	0.38	3.40	11.80
5.0	0.42	2.00	9.92
6.0	0.24	0.77	4.26
7.0	0.063	0.42	2.74
8.0	0.088	0.25	1.62
9.0		0.095	0.49
10.0			0.23
11.0			0.13

assuming a coalescence of the produced Λ hyperons with spectators. However, their rapidity cut is much larger ($(y_{proj} - 0.4) \leq \delta y_{\text{QMD}} \leq (y_{proj} + 0.4)$), than that used in our calculations. Therefore, we investigate within HIJING/B \bar{B} v2.0 model the sensitivity of our predictions to different rapidity cuts δy . An increase of δy from 0.05 to $\delta y = 0.5$ results in an increase of a factor 6-8 for the average value $\langle n_{\Lambda}(b) \rangle$. The sensitivity to the mean values of the in medium string tension (κ) is less important. Using Set 3 from Table I which correspond to a mean value $\kappa = 3$ GeV/fm, result in a modest increase (less than 3 – 5%) of $\langle n_{\Lambda}(b) \rangle$, for Ne + Ne central collisions ($b = 3$ fm) at $\sqrt{s_{NN}} = 5$ GeV.

Finally, for the symmetric colliding system $^{12}\text{C} + ^{12}\text{C}$, we investigate also the energy dependence of particle production for central collisions ($b = 3$ fm). When $\sqrt{s_{NN}}$ increase from 3.7 GeV to 5 GeV, the number of Λ particles ($\langle n_{\Lambda}(b) \rangle$) within kinematic cuts discussed above, has a modest increase of only 32%. The model predict a

more dramatic increase of $\langle n_{\Lambda}(b) \rangle$, i.e., a factor of 2.75 when $\sqrt{s_{NN}}$ increase from 5 GeV to 10 GeV. Since the energy range of the onset of deconfinement is expected to be at $\sqrt{s_{NN}} = 6-8$ GeV, the above energy range (5-10 GeV) should be carefully investigated by the future planned experiments.

III. MODEL FOR HYPERNUCLEUS FORMATION IN THE PLF

The Λ particles with appropriate rapidity find themselves in the PLF's. They thermalise along with the nucleons. In an event the Λ hyperon can remain unattached to nucleons or can combine with some nucleons to form a hypernucleus. There will be also “normal” composites, those without strangeness. Assuming equilibration we can compute the average numbers of both normal composites and hypernuclei. Past experience has shown that the temperature in the PLF is expected to be in the range of 5 to 8 MeV [32, 33].

The Canonical Thermal Model (CTM) for two kinds of particles (neutron and proton) has had long usage [45]. The extension to three kinds of particles (neutron, proton and Λ) was discussed by us in Ref. [20]. In this analysis we just give the details necessary to follow the calculations performed here. In CTM we need to calculate the partition function Q :

$$Q_{A_F, Z, H} = \sum \prod \frac{(\omega_{a, z, h})^{n_{a, z, h}}}{n_{a, z, h}!} \quad (4)$$

where A_F is the number of nucleons in the PLF plus one (the Λ particle); Z is the number of protons in the PLF and $H = 1$ (only one Λ with appropriate kinematic cuts discussed in Sec. II entered the PLF); $h = 0$ (normal composites) or $h = 1$, a hypernucleus; $\omega_{a, z, h}$ is the partition function of one composite with quantum numbers a, z and h ; $n_{a, z, h}$ is the number of this composite in a given channel. The sum in the above equation includes an enormous number of channels which satisfy conservation of quantum numbers:

$$\begin{aligned} \sum a n_{a, z, h} &= A_F \\ \sum z n_{a, z, h} &= Z \\ \sum h n_{a, z, h} &= H \end{aligned} \quad (5)$$

It is shown in Ref. [20] that the average occupation of (a, z, h) is given by:

$$\langle n_{a, z, h} \rangle = \frac{1}{Q_{A_F, Z, H}} \omega_{a, z, h} Q_{A_F - a, Z - z, H - h} \quad (6)$$

The partition functions Q can be calculated using recursion relations discussed in Ref. [20].

The one particle partition function $\omega_{a, z, h}$ has two parts:

$$\omega_{a, z, h} = z_{kin}(a, z, h) z_{int}(a, z, h) \quad (7)$$

The kinetic part is given by

$$z_{kin}(a, z, h) = \frac{V}{h^3} (2\pi MT)^{3/2} \quad (8)$$

where V is the freeze-out volume in which thermodynamics is assumed. For an atomic mass a we take V as 3 times the normal nuclear volume ($V_0 = a/\rho_0$, with $\rho_0 \approx 0.15 \text{ fm}^{-3}$), but then this volume is reduced for Van der Waals excluded volume ($V = 2V_0$). The mass of the composite M is: $M = (a - h)m_n + hm_\Lambda$, where m_n (938 MeV) and m_Λ (1116 MeV) stand for the nucleon mass and Λ mass respectively.

The internal partition function, $z_{int}(a, z, h)$ could be written as:

$$z_{int}(a, z, h) = \sum_i (2s_i + 1) \exp(-\beta e_i) \quad (9)$$

where e_i are energy eigenvalues of the composite (a, z, h) . However, considerable caution is needed in taking the sum over the energy states i . Because of Levinson's theorem the sum needs to be modified and cut off (see the discussion on Ref. [46]). In the previous work [20] the interest was to investigate gross features and a relative production only was discussed. Therefore, a generic formula for ground state binding energy and excited states was used for most nuclei.

In this analysis we are attempting a more quantitative estimate for production cross sections of hyperfragments ${}^A_F Z$ for $Z = 1$ to 4. The calculated cross sections differ significantly if we use the generic formula from Ref. [20], or experimental energies for ground and excited states. In the calculations performed here we have taken experimental values of ground state and excited state energies for low mass hypernuclei ($a < 11$). We include only particle stable excited states. The binding energies of ground

states for composites with strangeness $(a, z, 1)$ are estimated from tabulated values of B_Λ and binding energy of normal composites $(a - 1, z, 0)$. Data for $a < 11$ are taken from Refs. [9, 47] and references therein. The details are:

- ${}^3_\Lambda\text{H}$: only 1 state with spin 1/2.
 - ${}^4_\Lambda\text{H}$: ground state with spin 0 and one excited state with spin 1 at 1.04 MeV excitation.
 - ${}^4_\Lambda\text{He}$: ground state with spin 0 and one excited state with spin 1 at 1.15 MeV excitation.
 - ${}^5_\Lambda\text{He}$: only ground state with spin 1/2.
 - ${}^6_\Lambda\text{He}$: ground state with spin 1.
 - ${}^6_\Lambda\text{Li}$: ground state with spin 1.
 - ${}^7_\Lambda\text{He}$: ground state with spin 1/2.
 - ${}^7_\Lambda\text{Li}$: ground state with spin 1/2, excited state spin 3/2 at 0.69 MeV, excited state spin 5/2 at 2.05 MeV, excited state spin 7/2 at 2.521 MeV, excited state spin 1/2 at 3.56 MeV.
 - ${}^7_\Lambda\text{Be}$: ground state with spin 1/2.
 - ${}^8_\Lambda\text{Li}$: ground state with spin 1, one excited state with spin 1 at 1.22 MeV excitation
 - ${}^8_\Lambda\text{Be}$: ground state with spin 1, one excited state with spin 1 at 1.22 MeV excitation.
 - ${}^9_\Lambda\text{Li}$: ground state with spin 3/2.
 - ${}^9_\Lambda\text{Be}$: ground state with spin 1/2 and excited states with spins 5/2 and 3/2 grouped at 2.93 MeV.
 - ${}^{10}_\Lambda\text{B}$: ground state with spin 1, excited states with spin 2 at 0.22 MeV, another with spin 2 at 2.47 MeV and a spin 3 at 2.70 MeV.
 - ${}^{10}_\Lambda\text{Be}$: experimental binding is used but excitation energies and spins are taken to be the same as for ${}^{10}_\Lambda\text{B}$ by appealing to isospin symmetry.
- For heavier hypernuclei ($a > 10$), a liquid-drop formula is used for ground state energy. This formula is taken from Ref. [19]. All energies are in MeV.

$$e_{a,z,h} = -16a + \sigma(T)a^{2/3} + 0.72z^2/(a^{1/3}) + 25(a - h - 2z)^2/(a - h) - 10.68h + 21.27h/(a^{1/3}) \quad (10)$$

where $\sigma(T)$ is the surface tension which is a function dependent on temperature:

$$\sigma(T) = 18 \left[\frac{T_c^2 - T^2}{T_c^2 + T^2} \right]^{5/4} \quad (11)$$

A comparative study of the above binding energy formula can be found in Ref. [19]. This formula also defines the drip lines. We include all nuclei within drip lines in constructing the partition function.

In order to calculate $z_{int}(a, z, h)$ we use the liquid-drop formula for $e_{a,z,h}$ and include also the contribution coming from the excited states. This results in a multiplicative factor $\exp(r(T)\text{Ta}/\epsilon_0)$, where $r(T) = 12/(12+T)$ is a correction term. For a detailed discussion of parameters

used in these formulae see Ref [48]. As temperature T increases, this correction slows down the increase of partition function $z_{int}(a, z, h)$ due to excited states. Similar correction has been used before [46, 49], although this is not important for the temperature range considered here. We note, that our calculations take into consideration the effects of the long-range Coulomb force in the Wigner-Seitz approximation [48].

Apart from hypernuclei, we need also to specify the partition function ω for normal composites ($h = 0$). For ${}^1\text{H}$, ${}^2\text{H}$, ${}^3\text{H}$, ${}^3\text{He}$, ${}^4\text{He}$, ${}^5\text{He}$, ${}^5\text{Li}$, ${}^6\text{He}$, ${}^6\text{Li}$ and ${}^6\text{Be}$ we use experimental ground state energy and no excited states. For atomic mass $a > 6$ we use the generic formula from Eq. 10 with $h = 0$ and consider also the contributions

from the excited states as described above.

The temperature (T) in the PLF is also an important parameter in our calculations and it is expected to have no dependence on the beam energy value (in the range of 3-10 GeV). Many data can be used to estimate the temperature and the range $T = 5$ MeV to $T = 8$ MeV is a reasonable one in describing these data [32], [45]. Our results show, that predicted cross sections can change considerably within this range of the input temperatures, since at lower temperature heavier hypernuclei are favored at the expense of lighter ones. The average occupation number $\langle n_{a,1} \rangle = \sum_z \Lambda^a z$ will first drop with a , go through a minimum and rise again (see Fig. 1 and Fig. 2 from Ref. [20]). This is the well-known U shape. As the temperature changes, the shape changes very quickly to a different one, where the occupation falls monotonically with increasing a . The temperature domain of 5 MeV to 8 MeV is precisely the range where this happens. As a results occupations of the heavier constituents in the PLF can change dramatically. These suggest that the relative populations of lighter hypernuclei could be a good “measure” of the temperature in the PLF. Such effects are also seen in our results discussed in the Sec. IV (see Table III), but the situation there is more complex, because of impact parameter dependence and the expected fluctuations on the nucleon numbers in the PLF.

We also note, that the PLF system is finite, and in this temperature range grand canonical model results differ drastically from those obtained within CTM model, which include additional constrains such as particles number conservation. The detailed comparison of the results obtained using both models can be found in Ref. [45].

IV. RESULTS AND DISCUSSIONS

This work presents the inclusive production cross sections of different types of hypernuclei for the symmetric colliding systems $^{12}\text{C} + ^{12}\text{C}$ at $\sqrt{s_{NN}} = 3.7$ GeV, $^{20}\text{Ne} + ^{20}\text{Ne}$ and $^{40}\text{Ar} + ^{40}\text{Ar}$ at $\sqrt{s_{NN}} = 5$ GeV. We assume that Λ particles with a rapidity cut δy and total momenta less than 250 MeV/c in the rest frame of the projectile will thermalises with the nucleons in the PLF and will produce hypernuclei. In all three cases studied here the following characteristics are common. Integration over impact parameter is important. The relevant quantity is the product $b \langle n_{\Lambda}(b) \rangle$ in Eq. 1. The peak of this function is not too sharp. For small impact parameters ($b < 4$ fm) the number of nucleons in the PLF is small and thus only light hypernuclei can be formed when the hyperon Λ is captured. For large impact parameters ($b \geq 4$ fm) the number of nucleons in the PLF is greater than in the above case, and both light and heavy hypernuclei are formed.

Previous theoretical studies through coalescence model [5, 6, 11, 12] predicted the cross sections of the order of few microbarn (μb). The inclusive cross sections obtained

TABLE III: Inclusive production cross sections (all values are in μb) for different types of hypernuclei for the colliding system $^{12}\text{C} + ^{12}\text{C}$ at $\sqrt{s_{NN}} = 3.7$ GeV. Our results (column 2 and 3) are compared with previous predictions obtained within coalescence model [9–11] at $\sqrt{s_{NN}} \approx 2.7$ GeV.

Model Hypernuclei	Coalescence	CTM ($T = 5$ MeV)	CTM ($T = 8$ MeV)
$^3_{\Lambda}\text{H}$	0.22	0.89	3.25
$^4_{\Lambda}\text{H}$	0.39	0.32	0.71
$^4_{\Lambda}\text{He}$	0.39	0.34	0.77
$^5_{\Lambda}\text{He}$	2.58	3.87	1.46
$^6_{\Lambda}\text{He}$	0.32	0.50	0.17
$^7_{\Lambda}\text{He}$	0.09	0.0009	0.004
$^6_{\Lambda}\text{Li}$	0.30	0.56	0.18
$^7_{\Lambda}\text{Li}$	0.24	26.88	0.85
$^8_{\Lambda}\text{Li}$	0.18	0.17	0.13
$^9_{\Lambda}\text{Li}$	0.05	0.00008	0.0004
$^7_{\Lambda}\text{Be}$	0.07	0.001	0.005
$^8_{\Lambda}\text{Be}$	0.15	0.18	0.13
$^9_{\Lambda}\text{Be}$	2.48	22.3	2.26
$^{10}_{\Lambda}\text{Be}$	0.33	0.02	0.018

in our model for different types of hypernuclei (as indicated) for the light colliding system $^{12}\text{C} + ^{12}\text{C}$ at $\sqrt{s_{NN}} = 3.7$ GeV are given in Table III for temperature $T = 5$ MeV (second column) and $T = 8$ MeV (third column) in comparison with coalescence model results (at $\sqrt{s_{NN}} \approx 2.7$ GeV) [5, 6, 11, 12]. One knows that the total cross section of nucleon-nucleon ($N - N$) scattering becomes nearly constant at approximately 40 mb for c.m. energies in the range 2.5-10 GeV, and in this energy region only 1% of the ($N - N$) scattering produces a baryon of strangeness 1. Also we note that there is an energy threshold of ≈ 1.6 GeV for Λ production in an elementary process of $NN \rightarrow \Lambda KN$. Therefore, we could consider this comparison as appropriate, since in the region $\sqrt{s_{NN}} = 2-4$ GeV, the Λ hyperons production is expected to have a modest increase. Moreover, for Ne + Ne collisions, the calculations with coalescence model [5] show that the hypernucleus formation cross sections have also a modest increase (by 30-50%), when $\sqrt{s_{NN}}$ increase from 2.04 GeV to 3.1 GeV (see Fig. 6 in Ref. [5]).

Our results are different from those reported within the coalescence model [5, 6, 11, 12] which was used often to estimate cross sections for hypernucleus formation in the PLF. Only for few isotopes (e.g., $^4_{\Lambda}\text{He}$, $^8_{\Lambda}\text{Li}$, $^8_{\Lambda}\text{Be}$) we obtain inclusive cross sections slightly different in comparison with those predicted by the coalescence model. It is worthwhile to highlight the important differences.

To understand the basic idea of the coalescence model, let us begin by first considering a PLF without a hyperon. It is excited (usually parametrized by a temperature) and breaks up (as is well established experimentally) into many fragments. The distribution of these fragments (F) in the PLF can be denoted by $\frac{d^3N^F}{d^3p_F}(\vec{p}_F)$. Usually this distribution is not calculated in the coales-

cence model for hypernucleus formation although in some version of the coalescence this could be attempted. In principle, this distribution should be taken from experiment. In the present problem, we have, in addition, a Λ particle with a momentum distribution. If the velocity of the fragment \vec{p}_F/m_F and the velocity of the Λ particle, $\vec{p}_\Lambda/m_\Lambda$ match they can coalesce into a hypernucleus. Thus the cross-section is given by the product of two distributions and an overlap factor which gives the probability that the Λ and F becomes the hypernucleus ${}_\Lambda F$ (see Eq. 15 in Ref. [5] and Eq. 11 in Ref. [6]). Note that the Λ plays a very passive role here. Practitioners of the coalescence model suggested that $\frac{d^3 N^F}{d^3 p_F}$ has to be taken from experiment. In the past applications of the coalescence model, experimental values of $\frac{d^3 \sigma^F}{d^3 p_F}$ were not used as not all of those needed for predicting hypernucleus production were experimentally available. A theoretical model parametrisation for $\frac{d^3 \sigma^F}{d^3 p_F}$ had to be employed. These parameterizations give (wrongly) finite values for inclusive cross-sections of ${}^5\text{He}$ and ${}^8\text{Be}$ nuclei and hence finite values for inclusive cross-sections formation for both ${}^6_\Lambda\text{He}$ and ${}^9_\Lambda\text{Be}$. But this is fortuitous, since ${}^5\text{He}$ and ${}^8\text{Be}$ nuclei are not bound systems by themselves [17, 50]. However, calculations based on a generalized mass formula for non-strange and hypernuclei predict the existence of several bound hypernuclei (e.g., ${}^6_\Lambda\text{He}$ and ${}^9_\Lambda\text{Be}$) whose normal cores are unbound [51, 52].

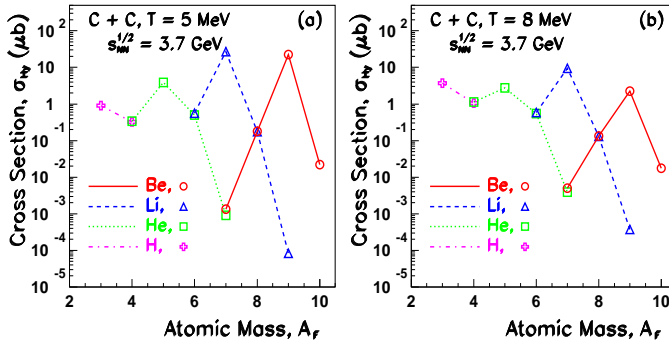


FIG. 2: (color online). The hypernucleus formation cross sections (σ_{Hy}) in ${}^{12}\text{C} + {}^{12}\text{C}$ collisions at $\sqrt{s_{NN}} = 3.7$ GeV as a function of nuclear fragment mass number A_r . The results (open symbols) are shown for H, He, Li and Be isotopes and are obtained for $T = 5$ MeV (left panel) and $T = 8$ MeV (right panel). The lines are only to guide the eyes.

These remarks lead to some features which are experimentally verifiable. For example, correct application of coalescence principles should give zero cross section for ${}^6_\Lambda\text{He}$ and ${}^9_\Lambda\text{Be}$ isotopes, since these require separately a ${}^5\text{He}$ nucleus and a Λ or a ${}^8\text{Be}$ nucleus and a Λ . The extra role the Λ play as “glue” ensuring stability, can not be incorporated in the coalescence model. In contrast in CTM model the Λ plays a more fundamental role than in coalescence. It participates in the thermalization. The CTM model uses directly the property of ${}_\Lambda F$ rather than that of F and Λ separately. Thus both ${}^6_\Lambda\text{He}$ and ${}^9_\Lambda\text{Be}$ are

expected to have non-zero production cross sections. In fact, we predict a large cross section for ${}^9_\Lambda\text{Be}$. The values obtained within our phenomenology are also shown in Fig. 2(a) ($T = 5$ MeV) and in Fig. 2(b) ($T = 8$ MeV). Note that the high value reported here for isotope ${}^7_\Lambda\text{Li}$ (on dashed lines) could be explained by many low-lying bound states of this isotope, which all contribute in the calculation of the partition function, z_{int} .

In collisions between heavy nuclei we expect an increase of the production rate of strangeness (see Table II in Sec. II) and of secondary interactions. In this case the temporal distribution of the fragment and Λ particle could play an important role and the reduction factors of about 0.5 was estimated with coalescence model [13] for ${}^{20}\text{Ne} + {}^{20}\text{Ne}$ at $\sqrt{s_{NN}} = 3.1$ GeV. Our results have been obtained by neglecting the above time dependence for ${}^{20}\text{Ne} + {}^{20}\text{Ne}$ and ${}^{40}\text{Ar} + {}^{40}\text{Ar}$ collisions at $\sqrt{s_{NN}} = 5$ GeV. Therefore, these values should be considered only as upper bounds for formation cross sections of hypernuclei. The predictions obtained within our hybrid model are shown through graphs in Fig. 3 and Fig. 4 (left panel, $T = 5$ MeV) and (right panel, $T = 8$ MeV).

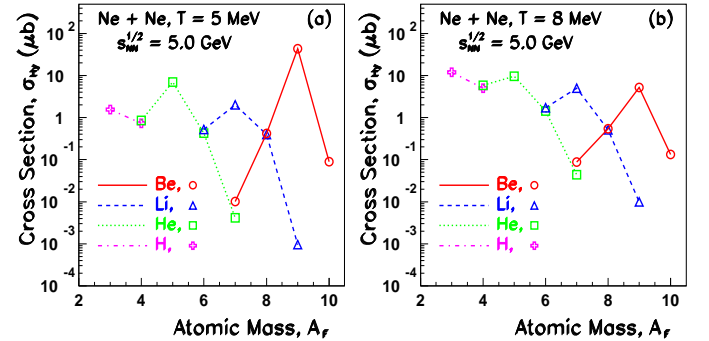


FIG. 3: (color online). The hypernucleus formation cross sections in ${}^{20}\text{Ne} + {}^{20}\text{Ne}$ collisions at $\sqrt{s_{NN}} = 5$ GeV. The open symbols and the lines have the same meaning as in Fig. 2.

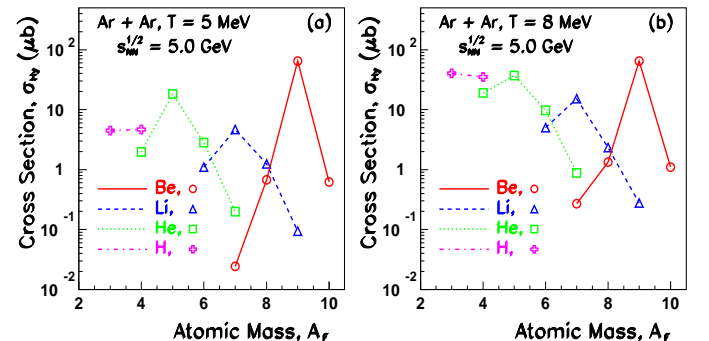


FIG. 4: (color online). The hypernucleus formation cross sections in ${}^{40}\text{Ar} + {}^{40}\text{Ar}$ collisions at $\sqrt{s_{NN}} = 5$ GeV. The open symbols and the lines have the same meaning as in Fig. 2.

The Ar + Ar system is twice as big as Ne + Ne (the total number of 80 nucleons versus 40). If we consider the results obtained for Li isotopes with $T = 5$ MeV (left

panel of Fig. 3 and Fig. 4), the graphs show that the hypernuclei formation cross sections are in Ar + Ar system approximately twice than those obtained in Ne + Ne system. In contrast, the production of ${}^9_{\Lambda}\text{Be}$ is about the same in both. One common feature of all three graphs (see Fig. 2, Fig. 3, Fig. 4) is that, the cross section for formation of ${}^9_{\Lambda}\text{Be}$ is large and is an order of magnitude higher than those predicted within coalescence model and this prediction should be easily verified by future experiments planned at FAIR and MPD/NICA.

Finally, we note that the previous experimental data for the production cross sections of ${}^4_{\Lambda}\text{H}$ and ${}^3_{\Lambda}\text{H}$ hypernuclei [2, 4] have been obtained with very light beams (He, Li) at 3.7A GeV (laboratory system) on carbon fixed target. We can not study using our approach these light colliding systems, since they are out of the limit of applicability within our phenomenology. To compare our predictions for formation cross sections of hypernuclei, data obtained with heavier beams (targets) and at higher energies are needed.

V. CONCLUSIONS

We have estimated the inclusive production cross-sections of selected light hypernuclei in the symmetric colliding systems (C + C, Ne + Ne, Ar + Ar) using a hybrid type model. The calculations are performed considering a product of two factors in impact parameter space (see Eq. 1). The first factor the average value per event, $\langle n_{\Lambda}(b) \rangle$, estimates the production of Λ particles in the participant region within a limiting phase space. Imposing reasonable kinematic cuts these particles could

be captured in PLF. The second factor, $\langle n_{a,z,1}(b) \rangle$, describes how these hyperons distribute them-self among the different hypernuclei within CTM approach. The absolute values of cross-sections are basically dependent upon the first part; the relative values are fixed by the canonical thermodynamic model (CTM). When data will become available, these can separately test the validity and accuracy of each part.

In comparison with previous predictions within coalescence models, our results show a striking difference especially for ${}^6_{\Lambda}\text{He}$ and ${}^9_{\Lambda}\text{Be}$ hypernuclei. A correct application of the coalescence principles should gives zero production cross sections for these isotopes. In contrast, our hybrid model predict a formation cross sections which are significantly larger than those reported with coalescence calculations.

Moreover, our approach for the production of hypernuclei in rHIC also applies with appropriate changes in rapidity and momentum cuts, to asymmetric colliding systems. However, to better test our predictions, experimental data obtained with heavier beams (target) and in the energy region of interest $\sqrt{s_{NN}} = 5\text{-}10$ GeV are required.

VI. ACKNOWLEDGMENT

We thank J. Barrette and M. Gyulassy for many fruitful and stimulating discussions. One of us (VTP) thanks M. Gyulassy for a pleasant hospitality at Columbia University, New York, where part of these calculations have been performed. This work was supported by the Natural Sciences and Engineering Research Council of Canada.

-
- [1] A. K. Kermann, M. S. Weiss, Phys. Rev. C **8**, 408 (1973).
 - [2] S. Avramenko *et al.*, Nucl. Phys. A**547**, 95c (1992).
 - [3] W. M. Alberico, G. Garbarino, Phys. Rep. **369**, 1 (2002).
 - [4] S. V. Averyanov *et al.*, Phys. of Atom. Nucl. **71**, 2101 (2008); Yad. Fiz. **71**, 2137 (2008).
 - [5] M. Wakai, H. Bando, and M. Sano, Phys. Rev. C. **38**, 748 (1988); M. Wakai, Nucl. Phys. A**547**, 89c (1992).
 - [6] F. Asai, H. Bando, and M. Sano, Phys. Lett. B **149**, 19 (1984).
 - [7] H. Bando, M. Sano, J. Zofka, and M. Wakai, Nucl. Phys. A**501**, 900 (1989).
 - [8] C. M. Ko, Phys. Rev. C **32**, 326 (1985).
 - [9] H. Bando, T. Motoba, and J. Zofka, Int. J. Mod. Phys. A **5**, 4021 (1990).
 - [10] H. Bando, Nuovo Cim. **102A**, 627 (1989).
 - [11] M. Sano and M. Wakai, Prog. Theor. Phys. Suppl. **117**, 99 (1994).
 - [12] H. Sato and K. Yazaki, Phys. Lett. B **153**, 153 (1981).
 - [13] M. Sano, ISN-Rep. **707**, (1988), *Lectures presented at the Lanzhou International Summer School on Heavy Ion Reaction Theory*, Lanzhou, August 10-18, 1988.
 - [14] A. J. Baltz, C. B. Dover, S. H. Kahana, Y. Pang, T. J. Schlagel, E. Schnedermann, Phys. Lett. **B325**, 7 (1994).
 - [15] Z. Rudy, T. Demski, L. Jarczyk, B. Kamys, P. Kulesza, A. Strzalkowski, W. Cassing, O. W. B. Schult, Z. Phys. A **351**, 217 (1995).
 - [16] W. Greiner, Int. J. Mod. Phys. E **5**, 1 (1995).
 - [17] C. Greiner, J. S. Bielich, arXiv:[nucl-th] 9801062, World Scientific Publication, Heavy Elements and Related New Phenomena, ed. by R. K. Gupta and W. Greiner (1998).
 - [18] R. Shyam, H. Lenske, U. Mosel, Nucl. Phys. **A764**, (2006).
 - [19] A. S. Botvina and J. Pochodzalla, Phys. Rev. C **76**, 024909 (2007).
 - [20] S. Das Gupta, Nucl. Phys. **A822**, 41 (2009).
 - [21] T. Gaitanos, H. Lenske, U. Mosel, Phys. Lett. B **675**, 297 (2009).
 - [22] HypHI Collaboration: Letter of Intent, <http://www.gsi.de/DOC-2005-Feb-432-2.pdf>.
 - [23] HypHI Collaboration: Progress Report, <http://www.gsi.de/DOC-2006-Jan-2-1.pdf>
 - [24] T. Saito, in *Proceedings of the IX International Conference on Hypernuclear and Strange Particle Physics (HyP 2006)*, Mainz, 2006, Ed. by J. Pochodzalla and Th. Wachter (SIF and Springer, Berlin, Heidelberg,

- 2007), p. 171
- [25] T. Fukuda and T. Saito, Nucl. Phys. **A790**, 161c (2007).
- [26] K. T. Brinkmann, P. Gianotti, and I. Lehmann, Nucl. Phys. News **16**, 15 (2006); arXiv:physics/0701090 (2007).
- [27] V. Friese for CBM Collaboration, Proceedings of Science (POS) **CPOD07**, 056 (2007).
- [28] V. Toneev, POS **CPOD07**, 057 (2007).
- [29] A. Sakaguchi *et al.*, arXiv:[nucl-th] 0904.0298 (2009).
- [30] STAR Collaboration, arXiv:[nucl-ex] 1003.2030 (2010).
- [31] S. Zhang, J. H. Chen, H. Crawford, D. Keane, Y. G. Ma, Z. B. Xu, Phys. Lett. **B684**, 224 (2010).
- [32] G. Chaudhuri and S. Das Gupta, Phys. Rev. C **75**, 034603 (2007).
- [33] J. B. Elliott *et al.*, Phys. Rev. C **67**, 024609 (2003).
- [34] X. N. Wang, M. Gyulassy, Comput. Phys. Commun. **83**, 307 (1994).
- [35] S. E. Vance and M. Gyulassy, Phys. Rev. Lett. **83**, 1735 (1999).
- [36] V. Topor Pop, M. Gyulassy, J. Barrette, C. Gale, X. -N. Wang, N. Xu, Phys. Rev. C **70**, 064906 (2004).
- [37] M. Gyulassy and A. Iwazaki, Phys. Lett B **165**, 157 (1985).
- [38] V. Topor Pop, M. Gyulassy, J. Barrette, C. Gale, Phys. Rev. C **72**, 054901 (2005);
- [39] V. Topor Pop, M. Gyulassy, J. Barrette, C. Gale, S. Jeon, R. Bellewied, Phys. Rev. C **75**, 014904 (2007).
- [40] N. Armesto *et al.*, J. Phys. G **35**, 054001 (2008); V. Topor Pop *et al.*, *ibidem*, pp 15-18; V. Topor Pop *et al.*, *ibidem*, pp 57-59.
- [41] V. Topor Pop, J. Barrette and M. Gyulassy, Phys. Rev. Lett. **102**, 232302 (2009).
- [42] J. S. Schwinger, Phys. Rev. **82**, 664 (1951).
- [43] E877 Collaboration, J. Barrette *et al.*, Phys. Rev. C **63**, 014902 (2001).
- [44] M. Gyulassy and V. Topor Pop (work in progress).
- [45] C. B. Das, S. Das Gupta, W. G. Lynch, A. Z. Mekjian, and M. B. Tsang, Phys. Rep. **406**, 1 (2005).
- [46] S. E. Koonin and J. Randrup, Nucl. Phys. **A474**, 173 (1987).
- [47] O. Hashimoto and H. Tamura, Prog. Part. Nucl. Phys. **57**, 564 (2006).
- [48] J. P. Bondorf, A. S. Botvina, A. S. Iljinov, I. N. Mishustin, and K. Sneppen, Phys. Rep. **257**, 133 (1995).
- [49] P. Bhattacharyya, S. Das Gupta and A. Z. Mekjian, Phys. Rev. C **60**, 054616 (1999).
- [50] E. Hiyama, T. Yamada, Prog. Part. Nucl. Phys. **63**, 339 (2009).
- [51] C. Samanta, P. Roy Chowdhury and D. N. Basu, J. Phys. G **32**, 363 (2006).
- [52] C. Samanta, P. Roy Chowdhury and D. N. Basu, J. Phys. G **35**, 06101 (2008).